

# On the Impact of Control Signaling in RIS-Empowered Wireless Communications

Fabio Saggese, *Member, IEEE*, Victor Croisfelt, *Student Member, IEEE*, Radosław Kotaba, Kyriakos Stylianopoulos, *Student Member, IEEE*, George C. Alexandropoulos, *Senior Member, IEEE*, and Petar Popovski, *Fellow, IEEE*

**Abstract**—The research on Reconfigurable Intelligent Surfaces (RISs) has dominantly been focused on physical-layer aspects and analyses of the achievable adaptation of the wireless propagation environment. Compared to that, questions related to system-level integration of RISs have received less attention. We address this research gap by analyzing the necessary control/signaling operations that are necessary to integrate RIS as a new type of wireless infrastructure element. We build a general model for evaluating the impact of control operations along two dimensions: *i*) the allocated bandwidth of the control channels (in-band and out-of-band), and *ii*) the rate selection for the data channel (multiplexing or diversity). Specifically, the second dimension results in two generic transmission schemes, one based on channel estimation and the subsequent optimization of the RIS, while the other is based on sweeping through predefined RIS phase configurations. We analyze the communication performance in multiple setups built along these two dimensions. While necessarily simplified, our analysis reveals the basic trade-offs in RIS-assisted communication and the associated control operations. The main contribution of the paper is a methodology for systematic evaluation of the control overhead in RIS-aided networks, regardless of the specific control schemes used.

**Index Terms**—Reconfigurable intelligent surfaces, control channel, protocol design, performance analysis.

## I. INTRODUCTION

Reconfigurable intelligent surfaces (RISs) constitute a promising technology for sixth generation (6G) wireless networks, which has received significant attention within the relevant research community in recent years [1]. The main underlying idea is to electronically tune the reflective properties of an RIS to manipulate the phase, amplitude, and polarization of the incident electromagnetic waves [2]. This creates a propagation environment that is, at least, partially controllable [3]. RISs can be fabricated with classical antenna elements controlled through switching elements or, more advanced, with metamaterials having tunable electromagnetic properties [4]. In the 6G context, the RIS technology has been identified as one of the cost-effective solutions to address the increasing demand for higher data rates, reduced latency, and increased coverage. In particular, an RIS can improve the received signal strength and minimize interference by reflecting signals to intended receivers and away from non-intended ones; this leads to applications aiming for increased

communication security [5] and/or reduced electromagnetic field exposure [6]. RISs can also extend the coverage of wireless communication systems by reflecting the signals to areas that are difficult to reach using conventional means [7].

The dominant part of the literature concerning RIS-aided communication systems deals with physical-layer (PHY) challenges. Recent studies have explored physics-based derivation of RIS-parametrized end-to-end channel models, incorporating causality, frequency selectivity, as well as any arising mutual coupling effects [8]. Many other papers have investigated the potential benefits of RIS-aided systems in terms of spectral and energy efficiencies by optimizing the parameters of the RIS' elements alone or jointly with the operations of the base station (BS) (see, *e.g.*, [9], [10]). To enable such strategies, several works have focused on designing and evaluating *channel estimation (CE) methods in the presence of RISs, either relying on the observed equivalent end-to-end channel from the BS to the user equipment (UE)*, when dealing with solely reflective RISs [11], [12], or directly estimating individual channels – BS-to-RIS and RIS-to-UE – by using simultaneous reflecting and sensing RISs [13]. The latter RIS design belongs to the attempts to minimize the CE overhead [14], which can be considerably large due to the expected high numbers of RIS elements [15] or hardware-induced non-linearities [9]. A different research direction bypasses explicit CE and relies on *codebook-based beam sweeping (CB-BSW) methods* [16]. Accordingly, the RIS is scheduled to progressively change among reflecting configurations from a predefined codebook so that the end-to-end system can discover the most suitable configuration [17]–[20]. The predefined codebook can be practically optimized for different purposes [21]: a suitable approach is to use hierarchical codebook structures [19], [22].

Within the existing research literature, the questions related to link/medium access control (MAC) protocol and system-level integration of RISs have received much less attention than PHY topics. *Specifically, the literature lacks a systematic treatment of the control signaling aspects, required to remotely manage the behavior of the RISs and the UEs. Control signaling is often exerted by the BS and relies upon well-defined control channels (CCs).* The study of those procedures is central to integrating RISs as a new type of network element within the existing wireless infrastructure. In this regard, we need to understand how the system performance is impacted by the design of the CCs in terms of its rate, reliability as well as the overhead/trade-offs incurred by the control signaling procedures. To the best of our knowledge, this paper marks the initial attempt to systematically investigate the influence of control signaling on the performance of RIS-aided wireless systems.

This work was partly supported by the Villum Investigator grant “WATER” from the Villum Foundation, Denmark, and by the EU H2020 RISE-6G project under grant number 101017011. F. Saggese, V. Croisfelt, R. Kotaba, and P. Popovski are with the Connectivity Section of the Department of Electronic Systems, Aalborg University, Aalborg, Denmark (e-mails: {fasa, vcr, rak, petarp}@es.aau.dk). K. Stylianopoulos and G. C. Alexandropoulos are with the Department of Informatics and Telecommunications, National and Kapodistrian University of Athens, Panepistimiopolis Ilissia, 15784 Athens, Greece (e-mails: {kstylianop, alexandrg}@di.uoa.gr).

### A. Related literature

Most of the existing literature assumes that the control over an RIS-aided communication system is error-free and instantaneous. For example, in [23] and later [7], the authors presented a detailed protocol for random access aided by an RIS. It was showcased that, despite the physical overhead of switching its configurations, the RIS brings notable performance benefits, allowing more UEs to access the BS on average. However, these works ignored the impact of control signaling. Similarly, in [24], the effect of re-transmission protocols in RIS-aided systems in the case of erroneous transmission was studied, but the control impact was ignored.

Other works did not even specify the required control information to be exchanged between the communication entities. For instance, one of the first works focusing on fast RIS programmability [17] presented a multi-stage CB-BSW protocol. By tasking the RIS to dynamically illuminate the area where a UE is located, the authors of [18] introduced a downlink (DL) transmission protocol, including UE localization, RIS configuration, and pilot-aided end-to-end CE. In [19], a fast near-field alignment scheme was proposed for the RIS phase-shifts and the transceiver beamformer, relying on a variable-width hierarchical RIS phase configuration codebook. Recently, [20] discussed the overhead and challenges of integrating the RIS into the network, arguing that the reduced overhead offered by CB-BSW schemes benefits the overall system performance. Nevertheless, the control signaling that needs to be exchanged for those schemes was not investigated.

### B. Contributions

This paper aims to introduce a model quantifying the impact of control signaling on the performance of RIS-enabled wireless communications. The number of actual control options is subject to a combinatorial explosion due to the system's large number of configurable parameters, such as frame size or feedback design. Obviously, we cannot address all these designs in a single work, but what we are striving for is to get a simple, yet generic, model for analyzing the impact of control that captures the essential design trade-offs and can be expanded to analyze other, more elaborate designs. For this reason, in this paper, we keep the complexity of the RIS-aided system model at the minimum, focusing on analyzing and evaluating the interaction between the control and the data planes. Considering a single-antenna BS and narrowband communications, we analyze the communication performance when control signaling occurs over the RIS-CC linking the BS to the RIS, and the UE-CC that links the BS to the UE through the RIS. To generalize the proposed model, we further discuss, at the end of the paper, how to relax some of the assumptions made. We build our generic control model along the two following dimensions that capture relevant trade-offs to be studied theoretically and which can be met in practice when deploying an RIS-aided communication system.

The *first dimension* is shaped around evaluating the distinctions between traditional communication paradigms of multiplexing and diversity [25]. In a *multiplexing-oriented transmission*, a key performance indicator (KPI) of interest – e.g., data

rate – is adapted to the actual channel conditions based on the channel state information (CSI) obtained via CE. However, CE generally needs complex control signaling, implying a high control overhead. In an RIS-aided system, for example, a multiplexing transmission corresponds to a case in which the RIS configuration is purposefully configured to maximize the signal-to-noise ratio (SNR) of the cascaded end-to-end channel, based on acquired CSI, and the data rate is chosen accordingly. In a *diversity transmission* scenario, the KPI is pre-established, and the UE relies on the expectation that the propagation environment will accommodate it. However, if the propagation environment does not meet these expectations, it can lead to an outage event, resulting in transmission failure. In an RIS-aided system, diversity transmission can be realized by using a CB-BSW procedure: while the UE transmits, the BS commands the RIS to successively load configurations, hoping that one of them will likely support the predefined KPI. We refer to the paradigm of RIS-aided multiplexing transmission as *optimization based on channel estimation (OPT-CE)*, while *CB-BSW* refers to the diversity paradigm.

The *second dimension* regards how the resources used by the CCs physically relate with the ones employed for the data channel (DC) used for data communication between the BS and UEs. We consider studying the following two options [26]. First, an *out-of-band CC (CC)* uses communication resources that are orthogonal to the ones used by the DC. More precisely, an OB-CC exerts control over the propagation environment but is not affected by this control. Second, an *in-band CC (CC)* uses the same communication resources as the DC. This implies that the IB-CC reduces the available resources to transmit data, likely decreasing the performance of the overall system. Furthermore, the successful transmission of the control messages toward the RIS depends on the current behavior of the RIS elements, meaning that the performance of the CC is now dependent on how the RIS is configured.

Our analysis suggests that employing either OPT-CE or CB-BSW depends on the specific service requirements and the coherence time of the DC. If the scenario exhibits high channel coherence time, the OPT-CE paradigm can potentially deliver superior data rate performance. However, its feasibility diminishes when the channel experiences rapid changes due to the increased control overhead. In contrast, the CB-BSW paradigm generally provides a lower data rate but proves suitable for scenarios with low coherence time due to its reduced control overhead. Additionally, our findings indicate that the reliability of control signaling is minimally affected by the paradigm used when the RIS-CC is an OB-CC. However, when an IB-CC serves as RIS-CC, the results reveal that OPT-CE control is less reliable than CB-BSW due to the increased complexity associated with the former in managing the RIS.

The paper is organized as follows. Section II presents the system model. Section III describes the transmission paradigms and their performance *assuming error-free CCs*. Section IV shows how to analyze the impact of CCs design in the communication performance, whose results are shown in Section V. Section VI discusses how to relax some of the simplification assumptions made in this paper, while Section VII concludes the paper.

*Notation:* Lower and upper case boldface letters denote vectors and matrices, respectively. Calligraphic letters denote sets, whose cardinality is  $|\cdot|$ . The Euclidean norm of  $\mathbf{x}$  is  $\|\mathbf{x}\|$ ;  $\odot$  denotes the element-wise product.  $\mathcal{P}(\cdot)$  is the probability of an event,  $\mathbb{E}[\cdot]$  is the expected value;  $\mathcal{CN}(\boldsymbol{\mu}, \mathbf{R})$  is the complex Gaussian distribution with mean  $\boldsymbol{\mu}$  and covariance matrix  $\mathbf{R}$ ,  $\text{Exp}(\lambda)$  is the exponential distribution with mean value  $1/\lambda$ .  $\lfloor a \rfloor$  is the nearest lower integer of  $a$ ;  $\mathbb{N}$  and  $\mathbb{C}$  are the set of natural and complex numbers;  $\Re\{\cdot\}$  returns the real part of a complex number, and  $j \triangleq \sqrt{-1}$ .

## II. SYSTEM MODEL

This section introduces a simplified communication model involving an RIS. We focus on the uplink (UL) scenario depicted in Fig. 1, which comprises a single-antenna BS, a single-antenna UE, and a solely reflective RIS [9]. The primary aim of this system is to facilitate efficient data communication between the UE and the BS with the support of the RIS. To accomplish this, the BS establishes control signaling links with both the RIS and the UE. The details and the key assumptions are given below.

*a) RIS operation model:* The internal operations of the RIS are divided into the RIS panel and the RISC. The panel comprises  $N$  elements equally spaced on a planar surface. The surface is solely reflective, implying that each element only controls the reflection properties of the incoming waves and that the RIS cannot process any of them. In particular, we focus on configuring the phases of the elements to change the reflection angle of an incoming wave, where their phase shifts are denoted as  $\varphi_n \in [0, 2\pi]$ ,  $\forall n \in \mathcal{N} = \{1, \dots, N\}$ <sup>1</sup>. We denote as  $\boldsymbol{\phi} = [e^{j\varphi_1}, \dots, e^{j\varphi_N}]^T \in \mathbb{C}^N$  the vector representing a particular *configuration*, i.e., the set of phase shifts configured at the metasurface's elements at a given time. The RISC is in charge of loading different configurations to the RIS surface. Without loss of generality, we indicate as  $\tau_s \in \mathbb{R}_+$  the time needed to switch to a new configuration. Moreover, the RISC is equipped with a communication module, which is used to exchange control signals with the BS. We refer to the link connecting the RISC to the BS as the RIS-CC. We consider that the RISC stores a look-up table containing a set of predefined configurations, namely the *common codebook* of configurations,  $\mathcal{C} = \{\phi_1, \dots, \phi_C\}$ ,  $|\mathcal{C}| = C$ , that can be designed according to the task at hand; a copy of  $\mathcal{C}$  is stored in the BS as well. The control signals between the BS and the RISC can then be based on indexing elements of  $\mathcal{C}$  or by explicitly sending a configuration  $\boldsymbol{\phi}$ , if the BS wants to load a configuration not present in the common codebook, i.e.,  $\boldsymbol{\phi} \notin \mathcal{C}$ . In the next sections,  $\mathcal{C}$  is going to be defined more explicitly according to OPT-CE and CB-BSW paradigms.

*b) UE communication model:* To analyze the communication performance, we assume a frame-based fixed time system of  $\tau \in \mathbb{R}_+$  seconds. The frame is further divided into phases that organize the signals exchanged at a given time.

<sup>1</sup>For the sake of simplicity and following the standard practice in literature, we consider an ideal RIS to show the theoretical performance achievable by the system at hand. We expect that more realistic models addressing attenuation, mutual coupling, quantization, and non-linear effects would reduce the overall performance [9].

Within a frame, control and data information are exchanged in different phases. In each frame, the UE communicate with the BS through the RIS: it transmits payload data using the UE-DC, while the exchange of control messages uses the UE-CC. To ensure mathematical tractability, ideal timing and frequency synchronization among devices at the PHY layer is assumed. Perfect synchronization is also considered at the frame level across these devices. Also, we consider that the RIS can be configured at any time within a frame, and we make the following assumption about the behavior of the RIS when the BS and the UE exchange control information.

**Assumption 1** (RIS ctrl configuration). *To allow control signaling exchange between the BS and the UE, we consider that the RIS loads a control (ctrl) configuration that ensures that control messages traveling through the UE-CC reach the destination<sup>2</sup>. Without loss of generality, we assume that the RISC loads the ctrl configuration when in idle, i.e., anytime it does not receive any explicit command from the BS.*

*c) Channel models:* We adopt the block fading model at a frame level, implying that the channel conditions remain constant throughout the frame duration. Remark that this binds the frame duration  $\tau$  to the channel coherence time: the higher the coherence time, the longer the frame duration. The following assumption is made on the channels, further described in the sequel.

**Assumption 2** (Narrowband channels). *To allow a simple analysis of both control and data channels, the three channels under consideration – 1) the UE-DC, 2) the UE-CC, and 3) the RIS-CC – are considered to be narrowband.<sup>3</sup>*

*1) UE-DC:* This channel operates at a central frequency  $f_d$  with a bandwidth of  $B_d$ . The UL SNR can be calculated as:

$$\gamma = \frac{\rho_u}{\sigma_b^2} |\boldsymbol{\phi}^T (\mathbf{h}_d \odot \mathbf{g}_d)|^2 = \frac{\rho_u}{\sigma_b^2} |\boldsymbol{\phi}^T \mathbf{z}_d|^2, \quad (1)$$

where  $\mathbf{h}_d \in \mathbb{C}^N$  and  $\mathbf{g}_d \in \mathbb{C}^N$  are the gains of UE-RIS and RIS-BS links, respectively. We further define the equivalent DC as  $\mathbf{z}_d = \mathbf{h}_d \odot \mathbf{g}_d \in \mathbb{C}^N$ . The UE transmit power is  $\rho_u$ , and  $\sigma_b^2$  is the noise power at the BS radio frequency (RF) chain<sup>4</sup>. The configurations  $\boldsymbol{\phi}$  supporting the UE-DC are subject to design and will be further specified in the following sections.

*2) UE-CC:* This channel operates at central frequency  $f_u$  with a bandwidth of  $B_u$ . The UE-CC channel is defined as

$$h_{cu} = \boldsymbol{\phi}_{\text{ctrl}}^T (\mathbf{h}_c \odot \mathbf{g}_c) = \boldsymbol{\phi}_{\text{ctrl}}^T \mathbf{z}_c, \quad (2)$$

where  $\boldsymbol{\phi}_{\text{ctrl}}$  is the ctrl configuration (see Assumption 1) and  $\mathbf{h}_c \in \mathbb{C}^N$  and  $\mathbf{g}_c \in \mathbb{C}^N$  are the gains of the UE-RIS and RIS-BS links, respectively. The equivalent end-to-end channel is

<sup>2</sup>The design of the ctrl configuration is out of the scope of this paper; potential candidates for ctrl configurations are wide-width beams and hierarchical radiation patterns, which generally offer good reliability and coverage when low data rates are needed [19], [27].

<sup>3</sup>The analysis can be straightforwardly extended to a wideband transmission, as discussed in Section VI.

<sup>4</sup>In the remainder of the paper, we assume that the BS knows the transmit and noise powers denoted through this section, i.e.,  $\rho_u$ ,  $\rho_b$ ,  $\sigma_b^2$ ,  $\sigma_u^2$  and  $\sigma_v^2$ ; the transmit powers are usually determined by the protocol or set by the BS itself; the noise powers can be considered static for a long time horizon and hence estimated previously through standard estimation techniques, e.g., [28].

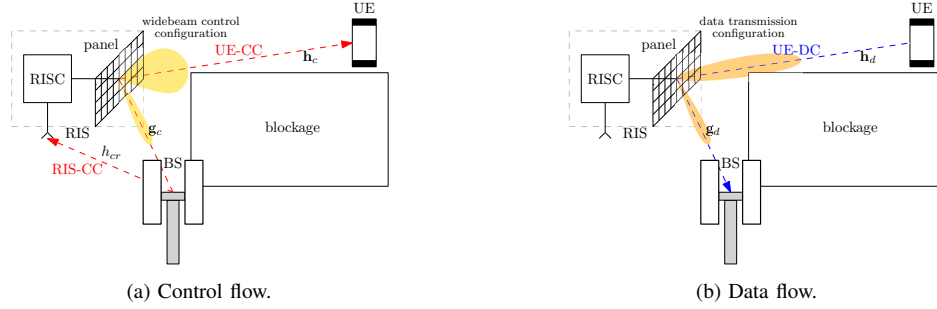


Fig. 1: Setup of interest: an RIS extends the coverage of the BS which has a blocked link to the UE. During control signaling, the RIS controller (RIS) loads a ctrl configuration to the RIS to deliver low-rate control packets to the UE. During data transmission, the BS controls and communicates with the RISC to load a certain configuration to achieve a desired communication performance.

$\mathbf{z}_c = \mathbf{h}_c \odot \mathbf{g}_c \in \mathbb{C}^N$ . We consider a worst-case scenario where the channel (2) has no line-of-sight (LoS) component, *i.e.*, it is distributed as  $h_{cu} \sim \mathcal{CN}(0, \tilde{\lambda}_u)$ ;  $\tilde{\lambda}_u$  is a term accounting for the large-scale fading – known by the BS – which is dependent on the ctrl configuration design. Hence, the instantaneous SNR measured at the UE is

$$\Gamma_u = \frac{\rho_b}{\sigma_u^2} |h_{cu}|^2 \sim \text{Exp}\left(\frac{1}{\lambda_u}\right), \quad (3)$$

where  $\lambda_u = \frac{\rho_b \tilde{\lambda}_u}{\sigma_u^2}$  denotes the average SNR at the UE, being  $\rho_b$  the BS transmit power and  $\sigma_u^2$  the UE's RF chain noise power. We make the following assumption on this channel.

**Assumption 3** (UE-CC design). *We assume that the UE-CC operates as an IB-CC, meaning that the frequency  $f_u$  matches the frequency  $f_d$ , and the physical resources allocated for the UE-CC coincide with those utilized for the UE-DC. This assumption is based on the premise that any UE-CC signal must travel through the RIS and the RIS operates at the same data frequency and bandwidth.*

3) *RIS-CC*: This narrowband channel operates on central frequency  $f_r$  with bandwidth  $B_r$ . Let  $h_{cr} \in \mathbb{C}$  denote the channel coefficient of the RIS-CC. To obtain simple analytical results, we assume that  $h_{cr} \sim \mathcal{CN}(0, \tilde{\lambda}_r)$ , where  $\tilde{\lambda}_r$  accounts for the large-scale fading, assumed known by the BS. Hence, the instantaneous SNR measured at the RISC is

$$\Gamma_r = \frac{\rho_b}{\sigma_r^2} |h_{cr}|^2 \sim \text{Exp}\left(\frac{1}{\lambda_r}\right), \quad (4)$$

where  $\lambda_r = \frac{\rho_b \tilde{\lambda}_r}{\sigma_r^2}$  denotes the average SNR with  $\sigma_r^2$  being the noise power at the RISC RF chain. We make the following assumption on the RIS-CC.

**Assumption 4** (RIS-CC design). *The RIS-CC can either be: i) IB-CC, implying that the physical resources employed by this channel are overlapping with the one used by the UE-DC, *i.e.*,  $f_r = f_d$ ; or ii) OB-CC, where the physical resources are orthogonal, *e.g.*, simulating a wired connection between the BS and the RISC. In the case of OB-CC, we further assume that the RIS-CC is an error-free channel, *i.e.*,  $\lambda_r \rightarrow \infty$ , with feedback capabilities since the system designer can easily make the RIS-CC as reliable as possible.*

### III. RIS-ENABLED COMMUNICATION PARADIGMS

In this section, we first describe the structure and building blocks of a generic RIS-enabled communication paradigm. We

use this to instantiate two particular transmission strategies: the OPT-CE and the CB-BSW, representing the multiplexing and diversity paradigms discussed in Section I-B. We analyze their performance in terms of the expected SNR and spectral efficiency (SE), while specifying the errors eventually occurring during their operations.

#### A. Generic structure

In a system without RISs, a generic structure for a typical transmission strategy can be divided into three key phases occurring in every frame: “*Signaling*,” “*Algorithmic*,” and “*Payload*.” The Signaling phase encompasses the actions conducted on the CCs required for network node control. This phase relies on the quality of the CCs and the information content within the control messages. The Algorithmic phase involves operations aiming at optimizing transmission parameters, such as selecting the transmit SE. The specifics of this phase are contingent on the chosen communication paradigm. The Payload phase handles the actual data transmission.

In an RIS-aided system, we identify that a generic structure would have two Signaling phases, namely “*Initialization*” and “*Setup*,” in conjunction with the “*Algorithmic*” and “*Payload*” phases. Sequentially, we have: Initialization, Algorithmic, Setup and Payload<sup>5</sup>. The time of a frame is thus divided as  $\tau = \tau_{\text{ini}} + \tau_{\text{alg}} + \tau_{\text{set}} + \tau_{\text{pay}}$ , where  $\tau_i < \tau$ , with  $i \in \{\text{ini, alg, set, pay}\}$ , is the time of the corresponding phase. The duration of each phase can vary depending on the paradigm and the kind of CCs. The phases are further elaborated as follows.

a) *Initialization*: The BS notifies the RIS and UE about the beginning of a frame over the CCs. It is assumed that the RISC loads the ctrl configuration at the start of this phase. Although not considered here, the Initialization phase can also incorporate a random access procedure (see, *e.g.*, [7]) as an intermediate step where newly connected UEs are scheduled.

b) *Algorithmic*: This phase encompasses all the processes and computations needed to optimize the subsequent Payload phase, where the actual data transmission takes place. Objectives of this phase encompass the selection/optimization of the appropriate RIS configuration(s), while others, such as

<sup>5</sup>We note that there could be communication strategies in which some of these phases may not be present, *e.g.*, access procedures; however, the mentioned four phases set a basis for a sufficiently general framework for RIS-aided communication that can be used, in principle, to design other schemes where some of the steps are merged or omitted, as discussed in Section VI.

determining the transmission parameters for the UE and/or the BS, could be included. To tackle these objectives, some form of wireless environment sensing from the end nodes is required, typically enabled by the transmission of pilot sequences, whose specifications – their number, waveform, UL or DL transmission, etc – are defined by the transmission strategy. The BS can then use the collected pilot signals and invoke pre-defined algorithms to fulfil the objectives. The outcome of these algorithms might be affected by different types of *algorithmic errors* that may prevent the system from performing as expected, and thus, should be considered when analyzing the overall performance.

*c) Setup:* During this phase, the RIS configuration chosen during the Algorithmic phase needs to be communicated to the RISC, which in turn commands the RIS to load it. Additionally, further control signaling may occur between the BS and the UE as a final check before data transmission to, e.g., set the modulation and coding scheme (MCS).

*d) Payload:* Here, the actual data transmission takes place while the RIS loads the configuration specified before. This phase may or may not include feedback of the data sent by the UE at the end; this aspect is not considered in this paper. The communication performance of the considered RIS-enabled communication system is measured during this phase.

In the following subsections, we describe two state-of-the-art paradigms using the generic structure defined above. After a general description, we investigate their Algorithmic phases, analyzing their performance and possible errors. The first paradigm is the *OPT-CE*, which follows a multiplexing transmission: the UE's CSI is evaluated at the BS and then exploited to compute the RIS' optimal configuration and the corresponding achievable data rate. Then, the transmission is made using the optimized configuration and MCS. The second approach is the *CB-BSW*, defined as a communication paradigm in [20], but already used in previous works (e.g., [18], [19], [23]). This paradigm resembles the concept of diversity transmission: the BS selects a target KPI *a priori*; then, it instructs the RISC to sweep through a set of predefined configurations, expecting that at least one will satisfy the target KPI; then, the transmission is made using the chosen configuration. Fig. 2 shows the data exchange diagrams of the two paradigms, comprised of CC messages, configuration loading, processing operations, and data transmission.

### B. Optimization based on Channel Estimation (OPT-CE)

In OPT-CE, the BS needs to obtain the CSI for the UE to optimize the RIS configuration. The necessary measurements can be collected by transmitting pilot sequences from the UE. During the Initialization phase, the BS informs the other entities that the procedure is starting. First, the UE is informed through the UE-CC to prepare to send pilots. Second, to solve the indeterminacy of the  $N$ -path CE due to the RIS presence [29], the RIS is instructed to sweep through a common codebook of configurations during the Algorithmic phase, called *CE codebook* and denoted as  $\mathcal{C}_{CE} \subseteq \mathcal{C}$ . To change between the configurations in the CE codebook, we consider that the BS needs to send only a single control

message to the RISC since the RIS sweeps following the order stipulated by the codebook. During the Algorithmic phase, the UE sends replicas of its pilot sequence, subject to different RIS configurations, to let each of them experience a different propagation environment. After a sufficient number of samples is received, the BS estimates the CSI and compute the optimal RIS's configuration [9]. Then, the Setup phase starts, in which the BS uses the the ctrl configuration<sup>6</sup> to implement the UE-CC and instruct the UE to start sending data. Subsequently, the BS informs the RISC, over the RIS-CC, to load the optimal configuration. Finally, the Payload phase takes place.

*1) Performance Analysis:* We now present the CE procedure and analyze its performance in connection to the cardinality of the employed codebook  $\mathcal{C}_{CE} = |\mathcal{C}_{CE}|$ . The considered method employed is a simplified version proposed in [29]. Let us start with the pilot sequence transmission and its processing. We denote a single pilot sequence as  $\psi \in \mathbb{C}^p$ , spanning  $p$  symbols and having  $\|\psi\|^2 = p$ . Every time a configuration from the codebook is loaded at the RIS, the UE sends a replica of the sequence  $\psi$  towards the BS. When the configuration  $c \in \mathcal{C}_{CE}$  is loaded, the following signal is received at the BS

$$\mathbf{y}_c^T = \sqrt{\rho_u} \phi_c^T \mathbf{z}_d \psi^T + \tilde{\mathbf{w}}_c^T \in \mathbb{C}^{1 \times p}, \quad (5)$$

where  $\phi_c$  denotes the phase profile vector of the configuration  $c \in \mathcal{C}_{CE}$ ,  $\rho_u$  is the transmit power, and  $\tilde{\mathbf{w}}_c \sim \mathcal{CN}(0, \sigma_b^2 \mathbf{I}_p)$  is the additive white gaussian noise (AWGN). The received symbol is then correlated with the pilot sequence and normalized by  $\sqrt{\rho_u p}$ , yielding

$$y_c = \frac{1}{\sqrt{\rho_u p}} \mathbf{y}_c^T \psi^* = \phi_c^T \mathbf{z}_d + w_c \in \mathbb{C}, \quad (6)$$

where  $w_c \sim \mathcal{CN}(0, \frac{\sigma_b^2}{p \rho_u})$  is the resulting AWGN.<sup>7</sup> The pilot transmissions and the processing in (6) are repeated for all RIS configurations, i.e.,  $\forall c \in \mathcal{C}_{CE}$ . The resulting signal  $\mathbf{y} = [y_1, y_2, \dots, y_{\mathcal{C}_{CE}}]^T \in \mathbb{C}^{\mathcal{C}_{CE}}$  can be then compactly written in the following form:

$$\mathbf{y} = \Theta^T \mathbf{z}_d + \mathbf{w}, \quad (7)$$

where  $\Theta = [\phi_1, \phi_2, \dots, \phi_{\mathcal{C}_{CE}}] \in \mathbb{C}^{N \times \mathcal{C}_{CE}}$  is the matrix containing all the configurations used and  $\mathbf{w} = [w_1, \dots, w_{\mathcal{C}_{CE}}]^T \in \mathbb{C}^{\mathcal{C}_{CE}}$  is the AWGN term. For the sake of generality, we will assume that there is no prior information about the channel distribution at the BS. Therefore, we cannot estimate separately  $\mathbf{h}_d$  and  $\mathbf{g}_d$ , but only the cascade channel  $\mathbf{z}_d$ . It is possible to show that a necessary (but not sufficient) condition to perfectly estimate the channel coefficients is that

<sup>6</sup>We remark that the ctrl configuration is automatically loaded after the Algorithmic phase ends due to the idle state of the RIS. Another approach is loading the optimal configuration evaluated in the Algorithmic phase also to send the control information toward the UE; nevertheless, the RISC needs to be informed previously by a specific control message by the BS. We do not consider this approach to keep the frame structure of the two paradigms similar, thereby simplifying the analysis and the presentation in Section IV.

<sup>7</sup>The consideration of dividing the pilot transmission over configurations over small blocks of  $p$  symbols serves three purposes: *i*) from the hardware point of view, it might be difficult to change the phase-shift profile of an RIS within the symbol time, *ii*) to reduce the impact of the noise, and *iii*) to have the possibility of separating up to  $p$  UE's data streams, if the pilots are designed to be orthogonal to each other [30].

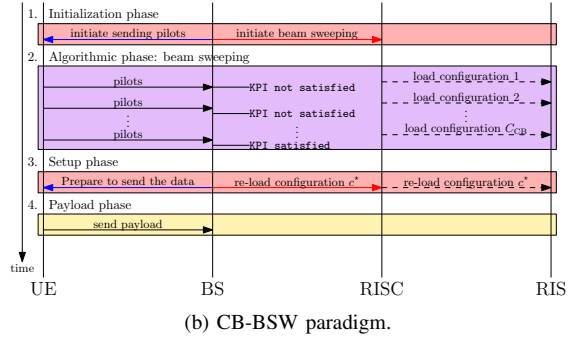
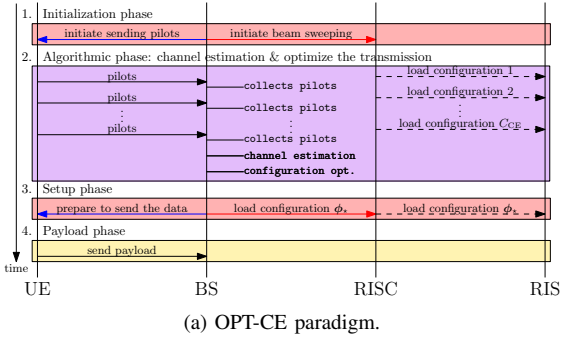


Fig. 2: Data exchange diagram of the two RIS-enabled communication paradigms. Signals traveling through RIS-CC, UE-CC, and UE-DC are represented by solid red, solid blue, and solid black lines, respectively. RISC to RIS commands are indicated with dashed black lines. BS operations are in monospaced font.

$C_{CE} \geq N$  [29]. Indeed, we want a linearly independent set of equations, which can be obtained by constructing the configuration codebook for CE to be at least of rank  $N$ . As an example, we can use the discrete Fourier transform (DFT) matrix, *i.e.*,  $[\Theta]_{n,c} = e^{-j2\pi \frac{(n-1)(c-1)}{C_{CE}}}$ , with  $n = \mathcal{N}$  and  $c \in \mathcal{C}_{CE}$ , with  $\Theta^* \Theta^T = C_{CE} \mathbf{I}_N$ . Considering that the parameter vector of interest is deterministic, the least-squares estimate yields the estimation [31]

$$\hat{\mathbf{z}}_d = \frac{1}{C_{CE}} \Theta^* \mathbf{y} = \mathbf{z}_d + \mathbf{n}, \quad (8)$$

where  $\mathbf{n} \sim \mathcal{CN}(0, \frac{\sigma_b^2}{C_{CE}} \mathbf{I}_N)$ , and whose performance is proportional to  $1/C_{CE}$ . Based on the estimated equivalent channel, the BS can obtain the configuration  $\phi_*$  that maximizes the instantaneous SNR of the typical UE, as follows:

$$\phi_* = \max_{\phi} \{ |\phi^T \hat{\mathbf{z}}_d|^2 \mid \|\phi\|^2 = N \}, \quad (9)$$

which turns out to provide the intuitive setting  $(\phi_*)_n = e^{-j\angle(\hat{\mathbf{z}}_d)_n}$ ,  $\forall n \in \mathcal{N}$ . The UL estimated SNR at the BS is:

$$\hat{\gamma}_{CE} = \frac{\rho_u}{\sigma_b^2} |\phi_*^T \hat{\mathbf{z}}_d|^2. \quad (10)$$

Based on the estimated SNR, the SE of the data communication can be adapted to be the maximum achievable, *i.e.*,

$$\eta_{CE} = \log_2(1 + \hat{\gamma}_{CE}). \quad (11)$$

2) *Algorithmic errors*: For the OPT-CE paradigm, a communication outage occurs in the case of an *overestimation error*, *i.e.*, if the selected SE  $\eta_{CE}$  is higher than the actual channel capacity, leading to an unachievable communication rate [32]. The probability of this event is

$$p_{ae} = \mathcal{P}[\eta_{CE} = \log_2(1 + \hat{\gamma}_{CE}) \geq \log_2(1 + \gamma_{CE})], \quad (12)$$

where  $\gamma_{CE} = \frac{\rho_u}{\sigma_b^2} |\phi_*^T \mathbf{z}_d|^2$  is the actual SNR at the BS. Eq. (12) translates to the condition

$$p_{ae} = \mathcal{P}[\hat{\gamma}_{CE} \geq \gamma_{CE}] = \mathcal{P}[|\phi_*^T \mathbf{z}_d + \phi_*^T \mathbf{n}|^2 \geq |\phi_*^T \mathbf{z}_d|^2]. \quad (13)$$

A detailed analysis of (13) relies on the channel model of  $\mathbf{z}_d$ , and thereby on a prior assumption about the scenario (*e.g.*, [33]); we therefore numerically evaluate the impact of the OPT-CE algorithmic error.

### C. Codebook-Based Beam Sweeping (CB-BSW)

In CB-BSW, the BS now does not require explicit CSI of the UE. In the Initialization phase, the BS commands the start of a new frame by signaling to the RIS and UE. A *beam sweeping (BSW) process*, *i.e.*, an RIS configuration selection, is performed during the Algorithmic phase. This process comprises the UE sending reference signals, while the BS commands the RIS to change its configuration at regular periods accordingly to a set of predefined configurations, labeled as the *BSW codebook* denoted by  $\mathcal{C}_{CB} \subseteq \mathcal{C}$ . The BS receives the reference signals that are used to measure UE's KPI. The BSW process is triggered when a single BS control message is received by the RISC. At its end, the BS selects a configuration satisfying the target KPI. During the Setup phase, the BS informs the UE over the UE-CC to prepare to send data, while the RIS uses the ctrl configuration, and informs the RISC through the RIS-CC to load the selected configuration. Finally, the Payload phase takes place.

**Remark 1** (Fixed vs Flexible frames). *The BSW process during the Algorithmic phase may make use of i) a fixed or ii) a flexible frame structure. The fixed frame ends after a fixed number of BSW codebook configurations have been loaded. The flexible frame structure allows stopping the BSW as soon as a KPI value measured is above the target one. Flexible frame requires on-the-fly KPI measurements at the the BS, while UE-CC needs to be reserved to promptly inform the UE about the frame termination when the target KPI is met, thus modifying the overall frame (see Section IV).*

1) *Performance analysis*: For CB-BSW it is necessary to assume that the target KPI is a target SNR  $\gamma_0$  measured at the BS via the average received signal strength (RSS) metric. In this case, a fixed SE is considered *a priori*, which is given by

$$\eta_{CB} = \log_2(1 + \gamma_0), \quad (14)$$

and the goal is find a configuration from the RIS codebook that supports it. We analyze the system performance starting from the pilot sequence transmission and processing. As before, every pilot sequence consists of  $p$  symbols<sup>8</sup>. Once again, we

<sup>8</sup>The pilot sequences for OPT-CE and CB-BSW can be different and have different lengths. In practice, they should be designed and optimized for each of those approaches, which is beyond the scope of this paper. We use the same pilot sequence length notation in both paradigms for simplicity.



denote a single sequence as  $\psi \in \mathbb{C}^p$  having  $\|\psi\|^2 = p$ . After the RIS loads configuration  $c \in \mathcal{C}_{\text{CB}}$ , the UE sends a replica of  $\psi$  and, similar to (5), the BS receives the signal:

$$\mathbf{y}_c^{\text{T}} = \sqrt{\rho_u} \phi_c^{\text{T}} \mathbf{z}_d \psi^{\text{T}} + \tilde{\mathbf{w}}_c^{\text{T}} \in \mathbb{C}^{1 \times p}, \quad (15)$$

where  $\phi_c$  denotes the configuration  $c \in \mathcal{C}_{\text{CB}}$ . The received signal is then correlated with  $\psi$  and normalized by  $p$ :

$$y_c = \frac{1}{p} \mathbf{y}_c^{\text{T}} \psi^* = \sqrt{\rho_u} \phi_c^{\text{T}} \mathbf{z}_d + w_c \in \mathbb{C}, \quad (16)$$

where  $w_c \sim \mathcal{CN}(0, \frac{\sigma_b^2}{p})$  is the resulting AWGN. The SNR provided by the configuration can be estimated as follows:

$$\hat{\gamma}_c = \frac{|y_c|^2}{\sigma_b^2} = \underbrace{\frac{\rho_u}{\sigma_b^2} |\phi_c^{\text{T}} \mathbf{z}_d|^2}_{\gamma_c} + 2\Re \left\{ \frac{\sqrt{\rho_u}}{\sigma_b^2} \phi_c^{\text{T}} \mathbf{z}_d w_c \right\} + \frac{|w_c|^2}{\sigma_b^2}, \quad (17)$$

where  $|w_c|^2 \sigma_b^{-2} \sim \text{Exp}(p)$ . It is worth noting that the estimated SNR is affected by the exponential error generated by the noise, but also by the error of the mixed product between the signal and the noise, whose probability distribution function (pdf) depends on the pdf of  $\mathbf{z}_d$ . Based on (17), we can select the best configuration  $c^* \in \mathcal{C}_{\text{CB}}$  providing the target KPI. According to Remark 1, we next discuss the selection of the configuration for the two different frame structures.

*a) Fixed Frame:* When the frame has a fixed structure, the BSW procedure ends after the RIS sweeps through the whole codebook. In this case, we can measure the KPIs for all available configurations. The configuration selected for the payload phase is the one achieving the highest estimated SNR among the ones satisfying the target KPI  $\gamma_0$ , as

$$c^* = \arg \max_{c \in \mathcal{C}_{\text{CB}}} \{\hat{\gamma}_c \mid \hat{\gamma}_c \geq \gamma_0\}. \quad (18)$$

If no configuration achieves the target KPI, the communication is not feasible, and we run into an outage event.

*b) Flexible Frame:* When the frame has a flexible structure, the end of the BSW process is triggered by the BS when the measured KPI reaches the target value. A simple on-the-fly selection method involves testing if the estimated SNR is greater than the target  $\gamma_0$ ; *i.e.*, after eq. (17) is obtained for configuration  $c \in \mathcal{C}_{\text{CB}}$ , we set

$$c^* = c \iff \hat{\gamma}_c \geq \gamma_0. \quad (19)$$

As soon as  $c^*$  is found, the BS communicates to both RIS and UE that the Payload phase can start; otherwise, the BSW process continues until a configuration is selected. If no configuration of the codebook  $\mathcal{C}_{\text{CB}}$  satisfies the condition (19), then communication is not feasible and outage occurs.

*2) Algorithmic errors:* For the CB-BSW paradigm, an outage event occurs when no configuration in the BSW codebook satisfies the target KPI, and when the selected configuration provides an SNR lower than the target one, although the estimated SNR was higher; we denote the latter as the overestimation event. These two events are mutually exclusive, and hence, their probability is

$$\begin{aligned} p_{\text{ae}} &= \mathcal{P}[\gamma_{c^*} \leq \gamma_0 \mid \hat{\gamma}_{c^*} > \gamma_0] + \mathcal{P}[\hat{\gamma}_c \leq \gamma_0, \forall c \in \mathcal{C}_{\text{CB}}] \\ &= \mathcal{P} \left[ \hat{\gamma}_{c^*} - \gamma_0 \leq \frac{|w_{c^*}|^2}{\sigma_b^2} + 2\Re \left\{ \frac{\sqrt{\rho_u}}{\sigma_b^2} \phi_{c^*}^{\text{T}} \mathbf{z}_d w_{c^*} \right\} \right] \\ &\quad + \mathcal{P}[\hat{\gamma}_1 \leq \gamma_0, \dots, \hat{\gamma}_{C_{\text{CB}}} \leq \gamma_0], \end{aligned} \quad (20)$$

where  $\gamma_{c^*} = \frac{\rho_u}{\sigma_b^2} |\phi_{c^*}^{\text{T}} \mathbf{z}_d|^2$  is the actual SNR and  $\hat{\gamma}_{c^*} - \gamma_0 > 0$ . By applying Chebychev inequality, the overestimation probability (first term) can be upper bounded by

$$\mathcal{P} \left[ \hat{\gamma}_{c^*} - \gamma_0 \leq \frac{|w_{c^*}|^2}{\sigma_b^2} + 2\Re \left\{ \frac{\sqrt{\rho_u}}{\sigma_b^2} \phi_{c^*}^{\text{T}} \mathbf{z}_d w_{c^*} \right\} \right] \leq \frac{p^{-1}}{\hat{\gamma}_{c^*} - \gamma_0}, \quad (21)$$

from which we infer that the higher the gap between  $\hat{\gamma}_{c^*}$  and  $\gamma_0$ , the lower the probability of error. The CB-BSW employing the fixed structure generally has a higher value of  $\hat{\gamma}_{c^*} - \gamma_0$  than the one with the flexible structure due to the use of the  $\arg \max$  operator to select the configuration  $c^*$ . Therefore, the fixed structure is generally more robust to overestimation errors. On the other hand, the evaluation of the probability that no configuration in the beam sweeping codebook satisfies the target KPI requires the knowledge of the cumulative density function (CDF) of the estimated SNR, whose analytical expression is channel-model dependent and generally hard to obtain. Here, we also resort to numerical evaluation of the impact of the CB-BSW algorithmic errors.

#### D. Trade-offs in different transmission paradigms

The two aforementioned RIS-aided transmission paradigms can be seen as a generalization of the *fixed rate* (multiplexing) and *adaptive rate* (diversity) transmission approaches. Essentially, the SE of the OPT-CE is adapted to the achievable rate under the optimal configuration (see (11)), while the SE of the CB-BSW is set *a priori* according to the target KPI (see (14)). Comparing (11) and (14) under the same environmental conditions, we have that

$$\eta_{\text{CB}} \leq \eta_{\text{CE}}, \quad (22)$$

where the price to pay for the higher SE of the OPT-CE paradigm is the increased overhead. OPT-CE needs an accurate CSI for reliable rate adaptation, which translates into a higher number of sequences to be transmitted by the UE compared to CB-BSW. Furthermore, additional time and processing are required to determine the optimal configuration of the RIS. Consequently, the SE of data transmission alone cannot be considered a fair comparison metric, as it does not consider the overheads generated by the communication paradigms.

#### IV. IMPACT OF THE CONTROL CHANNELS

In this section, we define a performance metric that simultaneously measures the communication performance and the impact of control signaling. We then characterize the terms of this metric regarding the overhead and the reliability of the signaling for the presented paradigms.

##### A. Utility function definition

To measure the communication performance, we define a utility function that takes into account *a)* the overhead and the error of the communication paradigms and *b)* the reliability of the CCs. Regarding the former, we define the *goodput*  $R$  as a discrete random variable whose value depends on the communication paradigm and its algorithmic errors:

$$R(\tau_{\text{pay}}, \eta) = \begin{cases} \frac{\tau_{\text{pay}}}{\tau} B_d \eta, & \text{with prob. } 1 - p_{\text{ae}}, \\ 0, & \text{with prob. } p_{\text{ae}}, \end{cases} \quad (23)$$

In this expression,  $\eta = \eta_{\text{CE}}$  in (11) or  $\eta = \eta_{\text{CB}}$  in (14) if OPT-CE or CB-BSW is respectively employed,  $\tau_{\text{pay}}$  is the duration of the payload phase, and  $\tau$  is the overall frame duration. The overall overhead time is the sum of the time to carry out the Initialization, Algorithmic, and Setup phases, denoted as  $\tau_{\text{ini}}$ ,  $\tau_{\text{alg}}$ , and  $\tau_{\text{set}}$ , respectively<sup>9</sup>. Accordingly, the payload time can be written as  $\tau_{\text{pay}} = \tau - \tau_{\text{ini}} - \tau_{\text{alg}} - \tau_{\text{set}}$ . While the overall frame length is fixed, the overhead time depends on the transmission paradigm, being a function of: the duration of a pilot,  $\tau_p$ , and the number of replicas transmitted; the optimization time,  $\tau_A$ ; and the time to control the RIS, composed of the time employed for the transmission of the control packets to the UE (RISC),  $\tau_i^{(u)}$  ( $\tau_i^{(r)}$ ), and the time needed by the RIS to switch configuration,  $\tau_s$ .

Regarding the reliability of the CCs, we denote as  $P = P_u + P_r$  the total number of control packets needed to let a communication paradigm work, where  $P_u$  and  $P_r$  are the numbers of control packets intended for the UE and the RIS, respectively. Whenever one of such packets is erroneously decoded or lost, an event of *erroneous control* occurs. We assume that these events are independent of each other (and of the algorithmic errors). We denote the probability of erroneous control on the packet  $i$  toward entity  $k \in \{u, r\}$  as  $p_i^{(k)}$ , with  $i \in \{1, \dots, P_k\}$  and  $k \in \{u, r\}$ . Erroneous controls may influence the overhead time and the communication performance: the RIS configuration might change unpredictably<sup>10</sup>, leading to a degradation of the performance, or worse, letting the data transmission fail. While losing a single control packet may be tolerable depending on its content, we assume all control packets must be received correctly to make the communication successful. In other words, no erroneous control event is allowed. Consequently, the probability of correct control is

$$p_{\text{cc}} = \prod_{k \in \{u, r\}} \prod_{i=1}^{P_k} (1 - p_i^{(k)}). \quad (24)$$

We can include the control reliability in the communication performance, taking into account the probability of correct control in the goodput metric in (23). By assuming that the control and algorithmic errors are independent, the goodput is re-expressed as follows:

$$R(\tau_{\text{pay}}, \eta) = \begin{cases} \frac{\tau_{\text{pay}}}{\tau} B_d \eta, & \text{with prob. } p_{\text{cc}}(1 - p_{\text{ae}}), \\ 0, & \text{with prob. } 1 - p_{\text{cc}}(1 - p_{\text{ae}}), \end{cases} \quad (25)$$

Hence, the performance of the considered RIS-enabled communication system can be described by averaging  $R$  w.r.t. the control, obtaining the following *utility function*:

$$U(\tau_{\text{pay}}, \eta) = p_{\text{cc}}(1 - p_{\text{ae}}) \left( 1 - \frac{\tau_{\text{ini}} + \tau_{\text{alg}} + \tau_{\text{set}}}{\tau} \right) B_d \eta. \quad (26)$$

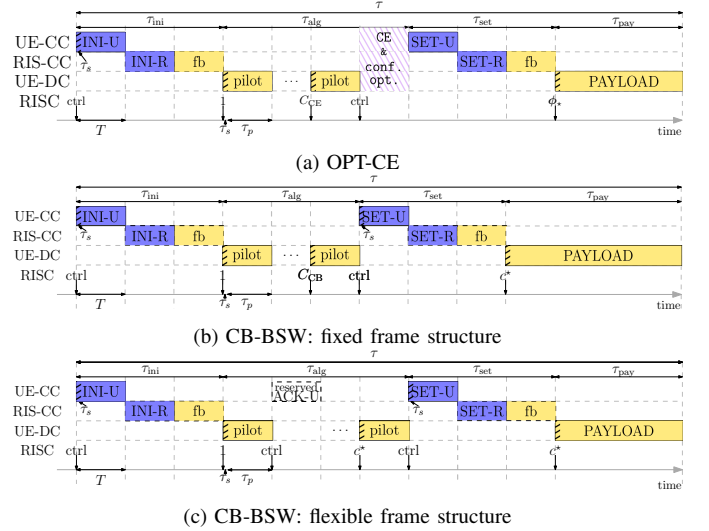


Fig. 3: Frame structure for the communication paradigms under study. Packets colored in blue and in yellow have DL and UL directions, respectively. Remark that INI-R (SET-R) packet and its feedback (fb) are sent at the same time as the INI-U (SET-U), but on different resources, if OB-CC is present (dashed lines).

## B. Overhead evaluation

Following the description of Section III, we present in Fig. 3 the frame structures of the two considered communication paradigms used to evaluate the induced overhead, where the rows represent the time horizon of the packets traveling on the different channels (first three rows) and the configuration loading time at the RISC (last row). The time horizon is obtained assuming that all the operations span multiple numbers of transmission time intervals (TTIs), each of duration of  $T$  seconds with  $\lceil \tau/T \rceil \in \mathbb{N}$  being the total number of TTIs in a frame. At the beginning of each TTI, if the RISC loads a new configuration, the first  $\tau_s$  seconds of data might be lost due to the unpredictable response of the channel during this switching period. When needed, we consider a guard period of  $\tau_s$  seconds in the overhead evaluation to avoid data disruption. Remember that the RISC loads the ctrl configuration any time it is in an idle state, *i.e.*, at the beginning of the Initialization and Setup phases.

In Fig. 3, we note that the overhead generated by the Initialization and Setup phases is *transmission paradigm independent*<sup>11</sup>, while it is *CC dependent*. Both paradigms make use of  $P = 4$  control packets,  $P_u = 2$  control packets sent on the UE-CC and  $P_r = 2$  on RIS-CC. Nevertheless, employing an OB-RIS-CC can reduce the overhead by transmitting the RIS control packets through orthogonal resources. On the other hand, the Algorithmic phase overhead is *CC independent* and *transmission paradigm dependent*, being designed to achieve

<sup>9</sup>We remark that the overhead time directly impacts on the latency experienced by the UE: given a fixed frame duration, a higher overhead translates into a lower time opportunity for the Payload phase, reducing the transmitted data in each slot, and hence, increasing the overall latency.

<sup>10</sup>In our scenario, if the control packet is not received, the RISC will load the ctrl configuration, *i.e.*, a predictable configuration change. However, if the RISC receives, but incorrectly decodes, a control packet, the BS cannot know which configuration, if any, will be loaded.

<sup>11</sup>The reliability is still dependent on the paradigm (see Section IV-C).



the goal of the specific paradigm regardless of the CC. In the following, the overhead is evaluated.

1) *Initialization phase*: This phase starts with the initialization control packet sent on the UE-CC (INI-U) informing the UE that the OPT-CE procedure has started. In the IB-CC case, this is followed by the transmission of the INI-R packet to the RISC to notify the beginning of the procedure. A consequent TTI for feedback is reserved to notify back to the BS if the INI-R packet has been received. If an OB-CC is employed, no TTI needs to be reserved because the INI-R and its feedback are scheduled simultaneously since the INI-U packet relies on different resources (see Assumption 4). The phase duration is  $\tau_{\text{ini}} = T$  or  $\tau_{\text{ini}} = 3T$  with OB- or IB-RIS-CC, respectively.

2) *Setup phase*: After the optimization has run, a setup (SET-U) packet spanning one TTI is sent to the UE notifying it to prepare to send the data; then, with an IB-CC, a TTI is used to send the SET-R packet containing the information of which configuration to load during the Payload phase; a further TTI is reserved for feedback. Again, if an OB-CC is present, the SET-R and its feedback are scheduled at the same time as the SET-U packet but on different resources; therefore, no TTIs needs to be reserved for the SET-R and its feedback. Remark that the  $\tau_s$  guard period must be considered by the UE when transmitting the data to avoid being disrupted during the load of the configuration employed in the Payload. For simplicity of evaluation, we account for this guard period in the Setup phase duration, resulting in  $\tau_{\text{set}} = \tau_{\text{ini}} + \tau_s$ .

3) *Algorithmic phase*: This phase comprises the process of sending pilot sequences and the consequent evaluation of the configuration for the transmission. Regardless of the paradigm, we assume each pilot sequence spans an entire TTI, but the configuration's switching time must be considered a guard period. Therefore, the actual time occupied by a pilot sequence is  $\tau_p \leq T - \tau_s$  and the number of samples  $p$  of every pilot sequence is given by  $p = \left\lfloor \frac{T - \tau_s}{T_n} \right\rfloor$ , where  $T_n$  is the symbol period in seconds. Assuming that the TTI duration and the symbol period are fixed, the UE can compute the pilot length if it is informed about the guard period. The overall duration of the Algorithmic phase depends on the paradigm employed.

a) *OPT-CE*: In this case, the Algorithmic phase starts with  $C_{\text{CE}}$  TTIs; at the beginning of each of them, the RISC loads a different configuration, while the UE transmits replicas of the pilot sequence. After all the sequences are received, the CE process at the BS starts, followed by the configuration optimization. The time needed to perform the CE and optimization processes depends on the algorithm and the available hardware. To consider a generic case, we denote this time as  $\tau_A = AT$ .

b) *CB-BSW fixed frame structure*: Similarly to the previous case, the Algorithmic phase starts with  $C_{\text{CB}}$  TTIs, at the beginning of which the RISC loads a different configuration, and the UE transmits replicas of the pilot sequence. After receiving all sequences, the BS selects the configuration as described in Section III-C. The time needed to select the configuration is considered negligible. Thus, the Setup phase may start in the TTI after the last pilot sequence is sent.

c) *CB-BSW flexible frame structure*: In this case, the number of TTIs used for the beam sweeping process is not

known *a priori* and depends on the measured SNR. However, to allow the system to react if the desired threshold is reached, a TTI is reserved for transmitting an acknowledgment (ACK-U) packet after each TTI used for pilot transmission. Hence, the number of TTIs needed is  $2c^* - 1$ , where  $0 < c^* \leq C_{\text{CB}}$  is a random variable.

Accordingly, the Algorithmic phase duration is

$$\tau_{\text{alg}} = \begin{cases} (C_{\text{CE}} + A)T, & \text{OPT-CE,} \\ C_{\text{CB}}T, & \text{CB-BSW fixed frame,} \\ (2c^* - 1)T, & \text{CB-BSW flexible frame.} \end{cases} \quad (27)$$

### C. Reliability evaluation

The reliability of the control packets depends on their informative content, the time reserved for their transmission, and the bandwidth of the CC. With equal transmission time and bandwidth, transmitting a high informative packet is less reliable than a low informative packet; similarly, increasing the time reserved leads to higher reliability. We account for this behavior via the outage probability of the  $i$ -the control packet intended to entity  $k \in \{u, r\}$ , which is given by

$$p_i^{(k)} = \Pr \left\{ \log(1 + \Gamma_k) \leq \frac{b_i^{(k)}}{\tau_i^{(k)} B_k} \right\}, \quad i = \{1, 2\}, \quad (28)$$

where  $i = 1, 2$  refers to the INI or SET packet, respectively;  $b_i^{(k)}$  is the amount of informative bits,  $\tau_i^{(k)}$  is the reserved time for transmission, and  $B_k$  is the CC bandwidth. Following the channel model in Section II, (28) can be rewritten as

$$p_i^{(k)} = 1 - \exp \left[ -\frac{1}{\lambda_k} \left( 2^{b_i^{(k)}/\tau_i^{(k)}/B_k} - 1 \right) \right]. \quad (29)$$

Plugging (29) into (24), the correct control probability is

$$p_{\text{cc}} = \exp \left[ \frac{1}{\lambda_u} \left( 2 - \sum_{i=1}^2 2^{b_i^{(u)}/\tau_i^{(u)}/B_u} \right) \right] \times \exp \left[ \frac{1}{\lambda_r} \left( 2 - \sum_{i=1}^2 2^{b_i^{(r)}/\tau_i^{(r)}/B_r} \right) \right]. \quad (30)$$

Remark that the informative content  $b_i^{(k)}$  and the reserved time  $\tau_i^{(k)}$  depend on the control packet and the communication paradigm employed due to the need to communicate different control information. Hence, different paradigms require different values of the average SNR of the UE-CC  $\lambda_u$  and the RIS-CC  $\lambda_r$  to obtain the same value of  $p_{\text{cc}}$ . In practice, the minimum  $\lambda_u$  and  $\lambda_r$  required to obtain the target correct control probability give a measure of the complexity of the decoding process. In the following, we compute  $\tau_i^{(k)}$  and  $b_i^{(k)}$  for the cases under investigation.

1) *Reserved time for control packets*: Each control packet spans an entire TTI following the data frame. However, the actual transmission time  $\tau_i^{(k)}$ , *i.e.*, the time in which informative bits can be sent without risk of being disrupted, depends on the RIS switching time. As discussed in Section IV-B, a guard period  $\tau_s$  must be considered if the RISC loads a new configuration in that TTI. Following the frame structure of Fig. 3, INI-R and SET-R packets can use the whole TTI,

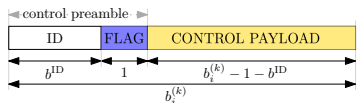


Fig. 4: General control packet structure.

while INI-U packets need the guard period. The SET-U control packet does not employ the guard period under the OPT-CE, as long as  $A \geq 1$ . The guard period is needed for the CB-BSW paradigm. Hence, the transmission time of the control packets intended for the UE is  $\tau_1^{(u)} = T - \tau_s$  for all paradigms, and  $\tau_2^{(u)} = T - \tau_s$  for CB-BSW and  $\tau_2^{(u)}$  for OPT-CE, while the time reserved for the control packets intended for the RISC is  $\tau_1^{(r)} = \tau_2^{(r)} = T$ .

2) *Control packet content*: Without loss of generality, we can assume a common structure for all the control packets, comprising a control preamble and a control payload as depicted in Fig. 4. The preamble comprises  $b^{\text{ID}}$  bits representing the *unique identifier (ID)* of the destination entity in the network and a single bit flag specifying if the packet is a INI or a SET one. From the preamble, the entity can understand if the control packet is meant to be decoded and how to interpret the control payload, whose informative bits depend on the kind of control packet and on the communication paradigm considered.

a) *OPT-CE*: To initialize the overall procedure at the UE, the payload of the INI-U packet must contain the length of the frame  $\tau$ , the cardinality of the set  $C_{\text{CE}}$ , and the guard time  $\tau_s$ . To simplify the data transmission, the frame duration can be notified through an (unsigned) integer  $b^{\text{frame}}$  containing the number of total TTIs  $\lceil \tau/T \rceil$  set for the frame. Similarly, we can translate the guard time into an unsigned integer representing the number of guard symbols  $\lceil \tau_s/T_n \rceil$  to send  $b^{\text{guard}}$  bits. Finally, another integer of  $b^{\text{conf}}$  bits can be used to represent the cardinality  $C_{\text{CE}}$  and to notify it to the UE. Its minimum value is  $b^{\text{conf}} = \lceil \log_2(C) \rceil$ , where  $C$  is the total number of configurations stored in the common codebook. Similarly, the payload of the INI-R packets needs to contain the information of the length of the frame  $\tau$ , and the *set* of configuration  $C_{\text{CE}}$  to switch through. The former uses the same  $b^{\text{frame}}$  bits of the INI-U packet. To encode the latter,  $b^{\text{conf}}$  bits are used to identify a single configuration in the common codebook, and thus,  $C_{\text{CE}} b^{\text{conf}}$  needs to be transmitted to the RISC, one per desired configuration. Regarding the Setup phase, the payload of the SET-U contains only the chosen SE of the communication  $\eta_{\text{CE}}$ . This can be encoded similarly to the MCS in the 5G standard [34]: a table of predefined values indexed by  $b^{\text{SE}}$  bits. The payload of the SET-R must contain the optimal configuration  $\phi_*$ , that is, a phase-shift value for each element. Without loss of generality, we denote by  $b^{\text{quant}}$  the number of bits used to control each element, *i.e.*, the level of quantization of the RIS [4]. Hence, the overall number of informative bits is  $Nb^{\text{quant}}$ . To summarize:

$$b_i^{(k)} = b^{\text{ID}+1} + \begin{cases} b^{\text{frame}} + b^{\text{guard}} + b^{\text{conf}}, & k = u, i = 1, \\ b^{\text{frame}} + C_{\text{CE}} b^{\text{conf}}, & k = r, i = 1, \\ b^{\text{SE}}, & k = u, i = 2, \\ Nb^{\text{quant}}, & k = r, i = 2. \end{cases} \quad (31)$$

TABLE I: Simulation parameters;  $\nu$  represents the speed of light.

Scenario		
Scenario side	$D$	20 m
BS position	$\mathbf{x}_b$	$(25, 5, 5)^T$ m
RIS element spacing	$d$	$\nu/f_d/2$
Number of RIS elements	$N$	100
Communication		
DC frequency	$f_d$	3 GHz
DC bandwidth	$B_d$	180 kHz
UE transmit power	$\rho_u, \rho_b$	24 dBm
UE/RIS noise power	$\sigma_u^2, \sigma_r^2$	-94 dBm
Paradigms		
Codebooks cardinality	$C_{\text{CE}}, C_{\text{CB}}^{\text{fix}}, C_{\text{CB}}^{\text{fle}}$	$N, \lceil N/3 \rceil, N$
Overall frame duration	$\tau$	[10, 200] ms
TTI duration	$T$	0.5 ms
Guard period	$\tau_s$	50 $\mu$ s
Pilot sequence length	$p$	1
CE duration in TTIs	$A$	5
Control packet content		
ID & Configuration bits	$b^{\text{ID}}, b^{\text{conf}}$	8
TTIs & Guard period bits	$b^{\text{frame}}, b^{\text{guard}}$	16
SE table bits	$b^{\text{SE}}$	6
RIS quantization level bits	$b^{\text{quant}}$	2

b) *CB-BSW*: The payload of the Initialization packets follows the same scheme used for the OPT-CE paradigm. The INI-U packet contains the length of the frame  $\tau$ , the cardinality of the set  $C_{\text{CB}}$ , and the guard time  $\tau_s$  in the (unsigned) integers  $b^{\text{frame}}, b^{\text{guard}}$ , and  $b^{\text{conf}}$ , respectively. The payload of the INI-R packets contains the information of the length of the frame  $\tau$ , and the *set* of configuration  $C_{\text{CB}}$  to switch through, encoded in the (unsigned) integers  $b^{\text{frame}}$  and  $C_{\text{CB}} b^{\text{conf}}$ , respectively. Instead, the Setup contains different information. In particular, the payload of the SET-U is empty, according to the fixed rate transmission used by this paradigm. The payload of the SET-R contains the configuration  $c^*$  encoded by the same  $b^{\text{conf}}$  bits, representing an index in the common codebook. To summarize, the packet length is:

$$b_i^{(k)} = b^{\text{ID}+1} + \begin{cases} b^{\text{frame}} + b^{\text{guard}} + b^{\text{conf}}, & k = u, i = 1, \\ b^{\text{frame}} + C_{\text{CB}} b^{\text{conf}}, & k = r, i = 1, \\ 0, & k = u, i = 2, \\ b^{\text{conf}}, & k = r, i = 2. \end{cases} \quad (32)$$

Remark that the informative content of the CB-BSW packets is lower or equal to the one of OPT-CE, leading the former to be more reliable than the latter.

## V. NUMERICAL RESULTS AND DISCUSSION

This section presents the performance evaluation of the communication paradigms under consideration.<sup>12</sup> The parameters set for the simulations are given in Table I, if not otherwise specified. The scenario is tested through Monte Carlo simulations. Concerning the scenario described in Section II, we consider that the BS and RIS positions  $\mathbf{x}_b$  and  $\mathbf{x}_r = (0, 0, 0)^T$  are kept fixed, while the UE position,  $\mathbf{x}_u$ , changes at every simulation according to a uniform distribution having limits

<sup>12</sup>The simulation code for the paper is available at <https://github.com/lostinafro/ris-control>.

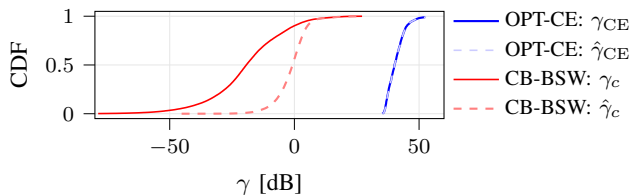


Fig. 5: CDF of the actual and estimated SNR for the communication paradigms under investigation.

$(-D/2, 0, 0)^T$  and  $(D/2, D, -D)^T$ . When referring to average performance, we implicitly assume averaging over different UE positions and noise realizations. The channel coefficients of the DC are evaluated considering the LoS component of  $\mathbf{h}_d$  and  $\mathbf{g}_d$  following the model of [35, Section II]. Note that the RIS-OB-CC uses a different operating frequency and bandwidth w.r.t. the DC ones, while, for the IB-CC, we have  $f_r = f_d$  and  $B_r = 5B_d$ . The UE-CC has operating frequency  $f_u = f_d$  and bandwidth  $B_u = 5B_d$ . The overall frame duration  $\tau$  reflects the coherence time of the channel: a low  $\tau$  represents a high mobility environment with low coherence time, and vice versa. The TTI duration is set according to the half of the subframe duration in the orthogonal frequency-division multiplexing (OFDM) 5G NR standard [34]. For the OPT-CE paradigm, the channel estimation codebook  $\mathcal{C}_{CE}$  is designed from the DFT, as described in Section III-B. For the sake of simplicity, the same configurations are used in the beam sweeping codebook  $\mathcal{C}_{CB}$ . In particular, the codebook used by the CB-BSW with flexible frame structure is  $\mathcal{C}_{CB}^{\text{fle}} = \mathcal{C}_{CE}$ , while the one used by the CB-BSW with fixed frame structure uses one every three configurations, to take advantage of the possible lower overhead. Next, we divide the results into two parts: evaluating the paradigms performance under error-free CCs and investigating the impact of CCs reliability.

#### A. Paradigms performance (error-free CCs)

Fig. 5 depicts the CDF of the actual and estimated SNRs to give some insight into the impact of the possible algorithm errors. From the figure, it can be inferred that the noise impact on the SNR estimation is generally negligible for the OPT-CE paradigm. This finding is justified by the fact that the power of the noise influencing the measurement is proportional to  $1/C_{CE}$ , where  $C_{CE} \geq N$  (see Section III-B). On the other hand, when employing the CB-BSW paradigm, the SNR is measured per each configuration, and the resulting noise has a higher impact on the estimation. Moreover, it can be observed that the SNR of the CB-BSW extends to very low values, while the minimum target KPI needs to be set to provide a non-negligible and supportable SE (at least higher than  $-13$  dB to reach the minimum SE value 0.0586 of 5G NR [36, Table 5.1.3.1-3]). Therefore, whatever reasonable target KPI is chosen, it will produce a relatively high outage probability. In summary, the OPT-CE paradigm is inherently more robust to algorithmic errors than the CB-BSW one.

To provide a fair comparison between the paradigms, we evaluate the optimal target SNR  $\gamma_0$  used as relevant KPI for the CB-BSW paradigm. Fig. 6 shows the average goodput  $R$  achieved as a function of the target SNR, under different kinds of CC and for different  $\tau$  values. We note that the

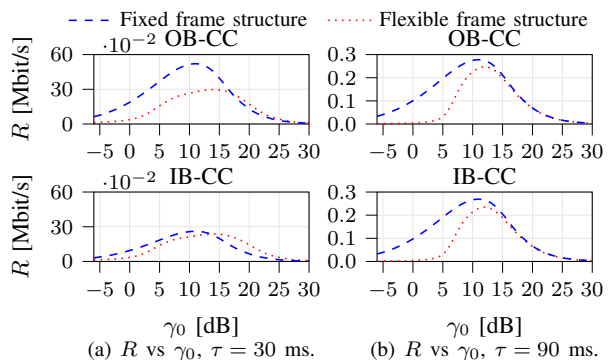


Fig. 6: Analysis of the target SNR for the CB-BSW paradigm (note the different scale in Fig. 6a).

optimal  $\gamma_0$  depends on the frame structure chosen, while it does not depend on the kind of CC. Moreover, the duration  $\tau$  influences negligibly the optimal  $\gamma_0$  in the flexible structure, being approximately 13.8 dB for  $\tau = 30$  ms and 12.4 dB for  $\tau = 90$  ms for the flexible frame structure, while approximately 10.9 dB for any value of  $\tau$  for the fixed frame structure. We remark that the selection of the target KPI is also scenario-dependent; hence, this procedure should be performed during the deployment of the RIS.

Using the optimal target SNR, we now compare the performance of the two paradigms. Fig. 7a illustrates  $R$  as a function of the overall frame duration. Again, the impact of the kind of CC on  $R$  is negligible. The main advantage of the CB-BSW approach is the possibility of providing a non-null transmission rate even in the presence of a lower coherence block ( $< 60$  ms), while the OPT-CE needs a longer time horizon to obtain the CSI and perform the Payload phase ( $\geq 60$  ms). On the other hand, as long as the time horizon is sufficiently long ( $\tau \geq 75$  ms), the OPT-CE paradigm outperforms the CB-BSW one. In Fig. 7b, we show the CDF of the goodput for  $\tau = 60$  ms. For this frame duration, the kind of CC influences the performance of the OPT-CE paradigm, while its impact is less predominant on the CB-BSW performance. As expected, the IB-CC performs worse due to its increased overhead. Nevertheless, for the CB-BSW, approximately half of the transmissions have null goodput because of algorithmic errors, while the OPT-CE provide a non-null goodput for all values, corroborating the results of Fig. 5.

#### B. Impact of the CCs reliability

Fig. 8 demonstrates the average utility (26) as a function of the erroneous control probability  $1 - p_{cc}$ , for  $\tau = 60$  ms and both kinds of CC. The results of the transmission paradigms are in line with the ones presented in Fig. 7. The CC reliability influences significantly the performance when  $1 - p_{cc} \leq 0.05$ , i.e.,  $p_{cc} \leq 0.95$ . To consider a conservative case, we set a target reliability to be  $\bar{p}_{cc} = 0.99$ , and we study the minimum average SNRs  $\lambda_u$  and  $\lambda_r$  providing such reliability, following the control packet content given in Table I. Fig. 9a shows the achieved  $p_{cc}$  for the OB-CC as a function of  $\lambda_u$  only, according to the assumption of error-free RIS-CC in the OB-CC case. With this kind of CC, the probabilities of correct control achieved by OPT-CE and CB-BSW have negligible

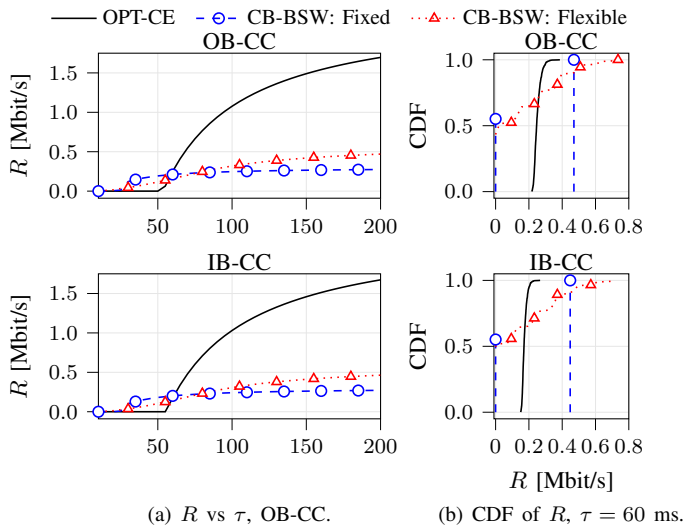


Fig. 7: Analysis of the goodput performance.

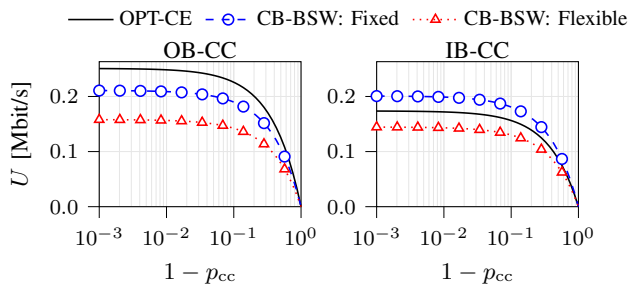


Fig. 8: Analysis of the utility function vs. erroneous control probability for  $\tau = 60$  ms.

differences, and  $\bar{\lambda}_u = 10.5$  dB is enough to provide the target correct control probability in both cases. Fig. 9b shows the  $p_{cc}$  as a heatmap function of  $\lambda_r$  and  $\lambda_u$  for the IB-CC case. Only the region satisfying the  $p_{cc} \geq 0.99$  is colored, and the minimum SNRs  $\bar{\lambda}_r$  and  $\bar{\lambda}_u$  needed are sketched. The OPT-CE needs higher SNRs than CB-BSW due to the higher information content of the control packets of the former. In particular, the need to transmit the phase-shift of each RIS element in the OPT-CE paradigm strongly impacts the overall reliability (see (31)). We remark that the performance provided by the CCs should be satisfied *simultaneously* to achieve the desired control reliability.

## VI. TOWARD MORE ELABORATE CONTROL DESIGNS

The presented performance analysis framework paves the way for the control signaling design and quantification of more sophisticated RIS-empowered wireless systems. It can be applied, for example, to multi-user wideband/OFDM communications [1], [2], by accounting for the subcarrier allocation of the different control and payload messages. For this system setup, the Algorithmic phase needs to also consider the resource allocation process, whose output should be signaled to the UEs through a specific design of the Setup phase. In addition, the current framework, by omitting, merging, or repeating some of its general phases, can set the basis for the control design in RIS-assisted networks with a multi-antenna BS and multi-antenna UEs, and smart wireless environments with multiple, possibly machine learning orches-

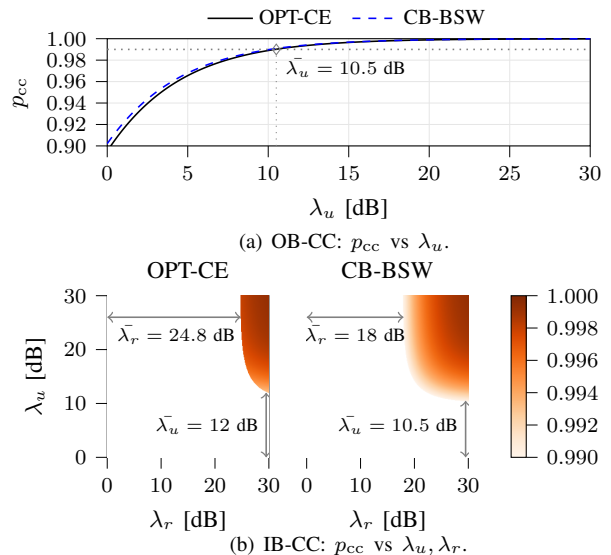


Fig. 9: Impact of the CC SNR on the reliability performance.

trated, RISs [37], as well as shared RISs among multiple communications pairs [4]. Of late interest are also multifunctional RISs [9], and especially those possessing sensing capabilities [14], which may provide higher flexibility for efficient control signaling designs [38].

We next elaborate in more detail on the case where the BS is equipped with multiple antennas and there exists the possibility of a weak direct link between itself and the UE. For the OPT-CE communication paradigm, the RIS configuration and the BS combiner can be jointly optimized [2], at the cost, of course, of a larger CE overhead and complexity, as well as larger algorithmic complexity. It is noted, however, that the increased beamforming gain from the multiple BS antennas might lead to cases where the BS-UE link is satisfactory, implying that the RIS deployment can be avoided, reducing the control overhead. For this mode to be realized, the operation protocol needs to enable, for example, the separate estimation of the UE-RIS-BS and UE-BS channels, via activation/deactivation of the RIS panel, as well as a relevant action during the Initialization phase. There exist various modes of operation when the CB-BSW paradigm is adopted. One is to perform BSW at the BS during the Initialization phase, together with BSW at the RIS, again at a cost of a larger overhead for both the fixed and flexible frame structures. Alternatively, to reduce the control signaling overhead, the BS combiner can be designed to solely match its channel with the RIS, or that with the UE if the RIS can be avoided, as discussed in the OPT-CE paradigm. One way to achieve the former is to capitalize on the common assumption that the RIS is placed such that there exists a strong line-of-sight with the BS [5]. In this way, the BS may adopt the reception configuration closest to maximal ratio combining. When the RIS can be avoided, the BS combiner can be similarly designed, now for the channel towards the UE - this operational mode can be decided similarly to the respective OPT-CE case.

It is finally noted that the two presented communication paradigms, namely OPT-CE and CB-BSW, can be combined to

devise additional signaling schemes. One example is presented in [18], where the CB-BSW is performed to set the RIS configuration when the link budget falls below a certain threshold, and then OPT-CE follows to set the BS combiner and/or the UE beamformer, treating the configured RIS as an unknown scatterer.

## VII. CONCLUSIONS

In this paper, we proposed a general framework of four phases (Initialization, Algorithmic, Setup, and Payload) to evaluate RIS-enabled communication performance while addressing the impact of control and signaling procedures. The data exchange and the frame structure for two different communication paradigms, namely OPT-CE and CB-BSW, were detailed. The performance of the paradigms was analyzed employing a utility function that considers the overhead generated by its various phases, the possible errors coming from the Algorithmic phase, and the impact of losing control packets needed for signaling purposes. Moreover, we particularized the performance evaluation for two kinds of CCs connecting the decision maker and the RISC – IB-CC and OB-CC –, showcasing the minimum performance needed to obtain the desired control reliability. Possible extensions of the proposed framework for more sophisticated scenarios of interest were discussed. Together with those extensions, in the future, we intend to study the impact of synchronization errors on the frame level and in the PHY-layer resources.

## REFERENCES

- [1] C. Huang *et al.*, “Reconfigurable intelligent surfaces for energy efficiency in wireless communication,” *IEEE Trans. Wireless Commun.*, vol. 18, no. 8, pp. 4157–4170, Aug. 2019.
- [2] Q. Wu *et al.*, “Intelligent reflecting surface aided wireless communications: A tutorial,” *IEEE Trans. Commun.*, vol. 69, no. 5, pp. 3313–3351, May 2021.
- [3] E. Calvanese Strinati *et al.*, “Reconfigurable, intelligent, and sustainable wireless environments for 6G smart connectivity,” *IEEE Commun. Mag.*, vol. 59, no. 10, pp. 99–105, Oct. 2021.
- [4] G. C. Alexandropoulos *et al.*, “RIS-enabled smart wireless environments: Deployment scenarios, network architecture, bandwidth and area of influence,” *EURASIP J. Wireless Commun. Netw.*, to appear, 2023.
- [5] —, “Counteracting eavesdropper attacks through reconfigurable intelligent surfaces: A new threat model and secrecy rate optimization,” *IEEE Open J. Commun. Society*, vol. 4, pp. 1285–1302, Jun. 2023.
- [6] N. Awarkeh *et al.*, “Electro-magnetic field (EMF) aware beamforming assisted by reconfigurable intelligent surfaces,” in *Proc. IEEE SPAWC*, Lucca, Italy, Sep. 2021.
- [7] V. Croisfelt *et al.*, “Random access protocol with channel oracle enabled by a reconfigurable intelligent surface,” *IEEE Transactions on Wireless Communications*, pp. 1–1, 2023.
- [8] R. Faqiri *et al.*, “PhysFad: Physics-based end-to-end channel modeling of RIS-parametrized environments with adjustable fading,” *IEEE Trans. Wireless Commun.*, vol. 22, no. 1, pp. 580–595, Jan. 2023.
- [9] M. Jian *et al.*, “Reconfigurable intelligent surfaces for wireless communications: Overview of hardware designs, channel models, and estimation techniques,” *Intell. Converged Netw.*, vol. 3, no. 1, pp. 1–32, Mar. 2022.
- [10] X. Cao *et al.*, “Massive access of static and mobile users via reconfigurable intelligent surfaces: Protocol design and performance analysis,” *IEEE J. Sel. Areas Commun.*, vol. 40, no. 4, p. 1253–1269, Apr. 2022.
- [11] A. L. Swindlehurst *et al.*, “Channel estimation with reconfigurable intelligent surfaces— A general framework,” *Proc. IEEE*, vol. 10, no. 9, pp. 1312–1338, Sep. 2022.
- [12] L. Mo *et al.*, “Direct tensor-based estimation of broadband mmWave channels with RIS,” *IEEE Commun. Lett.*, vol. 27, no. 7, pp. 1849–1853, Jul. 2023.
- [13] H. Zhang *et al.*, “Channel estimation with hybrid reconfigurable intelligent metasurfaces,” *IEEE Trans. Commun.*, early access, 2023.
- [14] G. C. Alexandropoulos *et al.*, “Hybrid reconfigurable intelligent metasurfaces: Enabling simultaneous tunable reflections and sensing for 6g wireless communications,” *arXiv preprint arXiv:2104.04690*, 2021.
- [15] V. Popov *et al.*, “Experimental demonstration of a mmWave passive access point extender based on a binary reconfigurable intelligent surface,” *Frontiers Commun. Netw.*, vol. 2, p. 733891, Oct. 2021.
- [16] C. Singh *et al.*, “Fast beam training for RIS-assisted uplink communication,” *arXiv preprint arXiv:2107.14138*, 2021.
- [17] B. Zheng and R. Zhang, “Intelligent reflecting surface-enhanced OFDM: Channel estimation and reflection optimization,” *IEEE Wireless Commun.*, vol. 9, pp. 518–522, 2020.
- [18] V. Jamali *et al.*, “Low-to-zero-overhead IRS reconfiguration: Decoupling illumination and channel estimation,” *IEEE Commun. Lett.*, vol. 16, no. 4, pp. 932–936, Apr. 2022.
- [19] G. C. Alexandropoulos *et al.*, “Near-field hierarchical beam management for RIS-enabled millimeter wave multi-antenna systems,” in *Proc. IEEE SAM*, Trondheim, Norway, 2022, pp. 460–464.
- [20] J. An *et al.*, “Codebook-based solutions for reconfigurable intelligent surfaces and their open challenges,” *arXiv preprint arXiv:2211.05976*, 2022.
- [21] M. Rahal *et al.*, “Performance of RIS-aided nearfield localization under beams approximation from real hardware characterization,” *EURASIP J. Wireless Commun. Netw.*, to appear, 2023.
- [22] J. Wang *et al.*, “Hierarchical codebook-based beam training for RIS-assisted mmWave communication systems,” *IEEE Trans. Commun.*, early access, 2023.
- [23] V. Croisfelt *et al.*, “A random access protocol for RIS-aided wireless communications,” in *Proc. IEEE SPAWC*, 2022.
- [24] S. Hao and H. Zhang, “Performance analysis of PHY layer for RIS-assisted wireless communication systems with retransmission protocols,” *J. Comp. Inf. Sciences*, vol. 34, no. 8, Part A, pp. 5388–5404, 2022.
- [25] P. Popovski, *Wireless Connectivity: An Intuitive and Fundamental Guide*, 03 2020.
- [26] E. Björnson *et al.*, “Reconfigurable intelligent surfaces: A signal processing perspective with wireless applications,” *IEEE Signal Process. Mag.*, vol. 39, no. 2, pp. 135–158, 2022.
- [27] M. He *et al.*, “RIS-assisted broad coverage for mmWave massive MIMO system,” in *Proc. IEEE ICC*, Montreal, USA, 2021.
- [28] T. Yucek and H. Arslan, “MMSE noise power and SNR estimation for OFDM systems,” in *Proc. IEEE Sarnoff Symposium*, Princeton, USA, 2006, pp. 1–4.
- [29] Z. Wang *et al.*, “Channel estimation for intelligent reflecting surface assisted multiuser communications: Framework, algorithms, and analysis,” *IEEE Trans. Wireless Commun.*, vol. 19, no. 10, pp. 6607–6620, 2020.
- [30] E. Björnson *et al.*, “Massive MIMO networks: Spectral, energy, and hardware efficiency,” *Foundations Trends Signal Process.*, vol. 11, no. 3–4, pp. 154–655, 2017.
- [31] S. M. Kay, *Fundamentals of Statistical Signal Processing: Estimation Theory*. Prentice Hall, 1997.
- [32] C. Shannon, “Communication in the presence of noise,” *Proceedings of the IRE*, vol. 37, no. 1, pp. 10–21, 1949.
- [33] D. Selimis *et al.*, “On the performance analysis of RIS-empowered communications over Nakagami- $m$  fading,” *IEEE Commun. Lett.*, vol. 25, no. 7, p. 2191–2195, 2021.
- [34] 3GPP, “Study on New Radio (NR) access technology,” 3rd Generation Partnership Project (3GPP), Technical Report (TR) 21.915, 10 2019, version 15.0.0.
- [35] A. Albanese *et al.*, “MARISA: A self-configuring metasurfaces absorption and reflection solution towards 6G,” in *Proc. IEEE INFOCOM*, 2022, pp. 250–259.
- [36] 3GPP, “NR; Physical layer procedures for data,” 3rd Generation Partnership Project (3GPP), Technical specification (TS) 38.214, 10 2022, version 15.0.0.
- [37] G. C. Alexandropoulos *et al.*, “Pervasive machine learning for smart radio environments enabled by reconfigurable intelligent surfaces,” *Proc. IEEE*, vol. 110, no. 9, p. 1494–1525, Sep. 2022.
- [38] V. Croisfelt *et al.*, “An orchestration framework for open system models of reconfigurable intelligent surfaces,” *arXiv preprint arXiv:2304.10858*, 2023.